Phosphatidylethanolamine critically supports internalization of cell-penetrating protein C inhibitor

Petra Baumgärtner,[1,2] Margarethe Geiger,[4] Susanne Zieseniss,[2] Julia Malleier,[4] James A. Huntington,[6] Karin Hochrainer,[4] Edith Bielek,[5] Mechthild Stoeckelhuber,[2] Kirsten Lauber,[7] Dag Scherfeld,[8] Petra Schwille,[8] Katja Wäldele,[1] Klaus Beyer,[3] and Bernd Engelmann[1,2]

[1]Vaskuläre Biologie und Hämostase, Institut für Klinische Chemie, 81377 Munich, Germany
[2]Physiologisches Institut, [3]Stoffwechselbiochemie, Ludwig-Maximilians-Universität, 80336 Munich, Germany
[4]Zentrum für Biomolekulare Medizin und Pharmakologie and [5]Zentrum für Anatomie und Zellbiologie, Medizinische Universität Wien, 1090 Vienna, Austria
[6]Division of Structural Medicine, Department of Haematology, University of Cambridge, Cambridge CB2 0XY, England, UK
[7]Medizinische Klinik I, Eberhard-Karls-Universität, 72076 Tübingen, Germany
[8]Max-Planck-Institut für Biophysikalische Chemie, 37077 Göttingen, Germany

Although their contribution remains unclear, lipids may facilitate noncanonical routes of protein internalization into cells such as those used by cell-penetrating proteins. We show that protein C inhibitor (PCI), a serine protease inhibitor (serpin), rapidly transverses the plasma membrane, which persists at low temperatures and enables its nuclear targeting in vitro and in vivo. Cell membrane translocation of PCI necessarily requires phosphatidylethanolamine (PE). In parallel, PCI acts as a lipid transferase for PE. The internalized serpin promotes phagocytosis of bacteria, thus suggesting a function in host defense. Membrane insertion of PCI depends on the conical shape of PE and is associated with the formation of restricted aqueous compartments within the membrane. Gain- and loss-of-function mutations indicate that the transmembrane passage of PCI requires a branched cavity between its helices H and D, which, according to docking studies, precisely accommodates PE. Our findings show that its specific shape enables cell surface PE to drive plasma membrane translocation of cell-penetrating PCI.

Introduction

Although endocytosis represents the prevailing route for the internalization of proteins into cells (D'Hondt et al., 2000; Itoh et al., 2001; Conner and Schmid, 2003), additional pathways have been suggested that only partially use or might even bypass the endocytic machinery. These pathways apparently facilitate the internalization of polybasic peptides such as magainin-2 and buforin (Matsuzaki et al., 1995, 1998; Takeshima et al., 2003), the HIV-1–based Tat protein, and the third helix of antennapedia from *Drosophila melanogaster* (penetratin), which mediates the transmigration of antennapedia through the plasma membrane and nuclear pore complex (Derossi et al., 1994; Joliot and Prochiantz, 2004). Although the mechanisms supporting cellular incorporation might vary among the different types of cell-penetrating peptides, membrane lipids could participate in several of the proposed pathways (Mäe and Langel, 2006). Lipids are indeed capable of directly supporting the membrane passage of proteins as shown for the release of (apo)cytochrome *c* from mitochondria (Diekert et al., 2001; Kuwana et al., 2002).

Distinctive properties of the lipid architecture of the cell membrane include lateral microdomains enriched in cholesterol and (glyco)sphingolipids, which constitute a platform for signal transmission and the internalization of microorganisms (rafts and caveolae; Simons and Vaz, 2004; Jacobson et al., 2007). Another key feature of the plasma membrane is represented by the transverse asymmetry of lipids. Under specific biological conditions, this asymmetry is attenuated, as exemplified by the surface exposure of phosphatidylserine (PS), which provides a recognition signal for the phagocytosis of apoptotic cells (Gardai et al., 2006) and establishes a catalytic surface for proteases implicated in blood coagulation (Bevers et al., 1999). Under the same

Correspondence to B. Engelmann: Bernd.Engelmann@med.uni-muenchen.de

P. Baumgärtner's present address is Ludwig Institute for Cancer Research, Division of Clinical Onco-Immunology, Lausanne, Switzerland.

B. Engelmann's present address is Institut für Klinische Chemie, Ludwig-Maximilians-Universität München, 81377 Munich, Germany.

Abbreviations used in this paper: CF, carboxyfluorescein; GUV, giant unilamellar vesicles; HC-II, heparin cofactor II; LUV, large unilamellar vesicles; NMR, nuclear magnetic resonance; PC, phosphatidylcholine; PCI, protein C inhibitor; PE, phosphatidylethanolamine; Pr^{3+}, praseodymium; PS, phosphatidylserine; rPCI, recombinant PCI; SUV, small unilamellar vesicles; uPCI, urinary PCI.

The online version of this paper contains supplemental material.

The Journal of Cell Biology, Vol. 179, No. 4, November 19, 2007 793–804
http://www.jcb.org/cgi/doi/10.1083/jcb.200707165

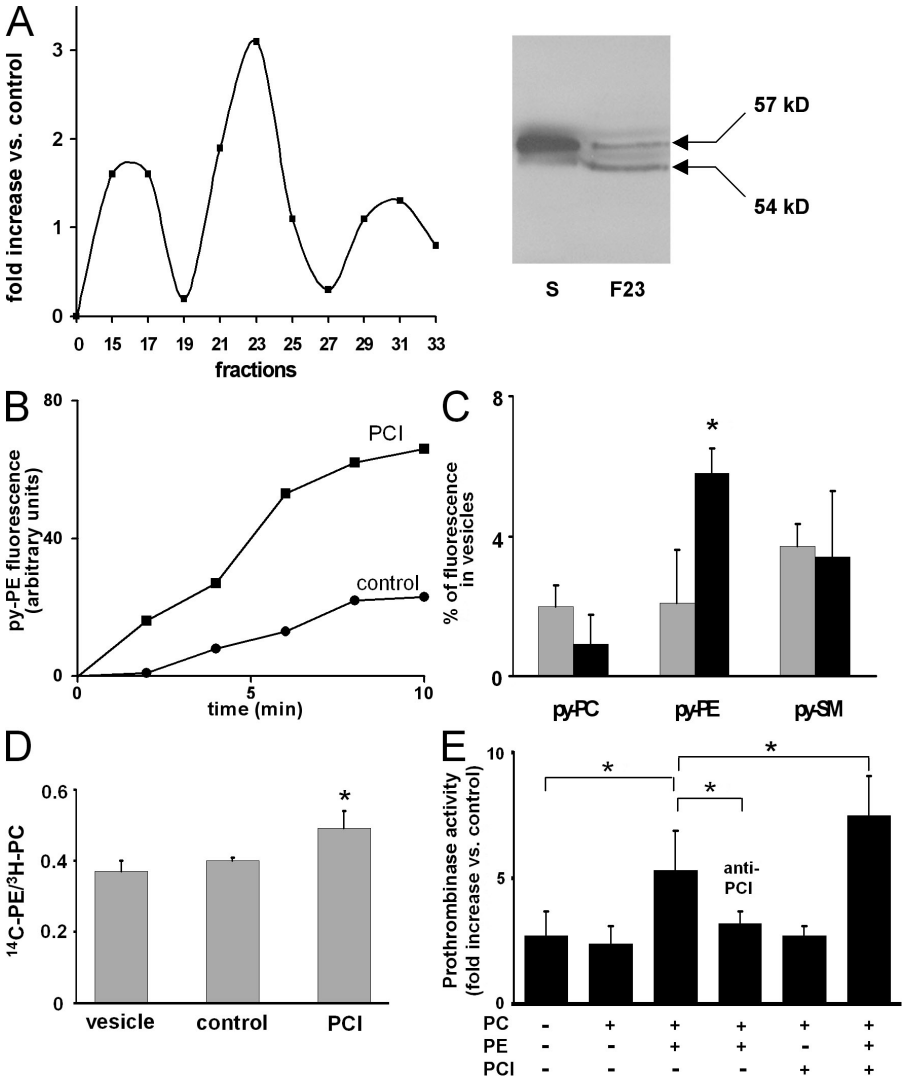

Figure 1. **Identification of PCI as a lipid transferase promoting the cellular import of PE.** (A) PCI is present in the platelet releasate fraction with the highest PE transfer activity. (left) Supernatants from thrombin-activated human platelets were separated by gel chromatography and the fractions were analyzed for their capacity to exchange py-PE between two types of SUV in vitro. (right) PCI is detected by a monoclonal anti-PCI antibody in the total supernatant (S) and fraction 23 (F23) exhibiting the highest py-PE exchange activity (57- and 54-kD forms of the serpin). (B) Acceleration of lipid exchange in vitro defines PCI as a PE transfer protein. The py-PE transfer from donor vesicles to unlabeled acceptor vesicles was registered in the absence (●) or presence of 20 nM uPCI (■). Similar findings were obtained with rPCI (not depicted). (C) PCI selectively enhances the cellular import of PE. Isolated human platelets were incubated at 37°C for 10 min with uPCI and SUV containing the indicated py-phospholipids. Gray, control; black, PCI. $n = 3–6$. *, $P < 0.05$. (D) PCI supports cell uptake of [^{14}C]PE. Platelet associated radioactivity was determined after incubation with SUV (95:5% PC/PE; ^{14}C-PE and ^{3}H-PC) without (control) or with uPCI (10 min, 37°C). $n = 5$. *, $P < 0.05$ versus vesicle and control. (E) Facilitation of PE transfer increases thrombin formation. Platelets were challenged with 0.5 U/ml thrombin, a relatively weak stimulator of the prothrombinase activity, which nevertheless induces a robust secretion of PCI. In the presence of SUV containing PC alone (PC) or 5% PE plus 95% PC (PE; mol%), thrombin generation by the prothrombinase complex was evaluated with or without uPCI. Control experiments verified that no prothrombinase activity was elicited by the PE vesicles in the absence of platelets. An isotype control antibody did not inhibit the prothrombinase activity of activated platelets in the presence of PC/PE vesicles (not depicted). $n = 4–6$. *, $P < 0.05$. Results show mean values ± SD.

conditions, the exposure of phosphatidylethanolamine (PE) is enhanced (Emoto et al., 1997; Smirnov et al., 1999). However, in contrast to the well-known functions of PS exposure, the functional meaning of PE externalization is largely unknown.

We found that the cellular internalization of the serpin protein C inhibitor (PCI) is crucially supported by plasma membrane PE, which enables its rapid targeting to the nucleus both in vitro and in vivo. Our findings position PCI as an eminent candidate for the nuclear supply of cargo. On the basis of the crystal structure of PCI, a hydrophobic cavity has been characterized as the binding site for PE, which is recognized by specific lipids of conical morphology. Our findings indicate cell surface PE as a mediator for the cell membrane translocation of proteins and suggest that this requires the ability of the lipid to foster formation of transient nonbilayer domains within the membrane.

Results

PCI acts as selective transferase for PE

The lipid structure of the plasma membrane can be dynamically regulated by the selective insertion of extracellular lipids via specialized proteins such as scavenger receptor class B type I, which transfers cholesterol and phospholipids into cells (Acton et al., 1996; Urban et al., 2000), CD14, a transporter for phosphatidylinositol (Wang and Munford, 1999), and the fatty acid carrier CD36 (Koonen et al., 2005). These also include unknown proteins mediating the cellular import of PE (Engelmann et al., 1998). To identify the latter proteins, we separated the supernatants from activated blood platelets by gel filtration. Then the phospholipid transfer activities of the fractions were measured by determining the exchange of fluorescent-labeled phospholipids between donor and acceptor vesicles. Among the fractions analyzed, fraction 23 caused the strongest stimulation of the intervesicular transfer of fluorescent-labeled PE (Fig. 1 A). Because activated platelets secrete the PE- binding serpin PCI (Nishioka et al., 1998; Prendes et al., 1999), we analyzed whether fraction 23 contained this protein. PCI could indeed be detected in the active fraction (Fig. 1 A). The serpin was additionally recovered in the total supernatant (Fig. 1 A). To evaluate whether PCI was principally capable of mediating the PE transfer through aqueous media, the serpin was added to suspensions of labeled donor vesicles and unlabeled acceptor vesicles.

Isolated PCI was found to transfer fluorescent-labeled PE to the acceptor vesicles within short time periods (Fig. 1 B), which documents that the serpin supports the intermembrane exchange of PE. Moreover, PCI markedly augmented the incorporation of extracellular fluorescent-labeled PE into platelets (Fig. 2 C) and several other cells (human monocytes, neutrophils, and umbilical vein endothelial cells; not depicted). However, PCI failed to enhance the incorporation of fluorescent-labeled phosphatidylcholine (PC), sphingomyelin (Fig. 1 C, SM), and PS (not depicted). The enhanced PE uptake by the activated platelets was almost completely abolished by the anti-PCI antibody (Fig. S1, available at http://www.jcb.org/cgi/content/full/jcb.200707165/DC1). Next, resting platelets were incubated with small unilamellar vesicles (SUV) containing 5% of total lipids on a molecular basis (mol%) of PE (reflecting the percentage of PE in human lipoproteins) and, additionally, [^{14}C]PE + [^{3}H]PC. In the absence of PCI, the [^{14}C]PE/[^{3}H]PC ratio remained unchanged compared with the ratio of the vesicles alone. In contrast, PCI augmented the [^{14}C]PE/[^{3}H]PC ratio, indicating that the serpin enhances [^{14}C]PE transfer into platelets (Fig. 1 D). Hence, PCI promotes phospholipid import at physiological concentrations of extracellular PE. Insertion of PE into the platelet cell membrane could influence the activity of the prothrombinase complex, which is known to be stimulated by cell surface PE (Billy et al., 1995). Platelets were challenged with thrombin, a relatively weak stimulator of the prothrombinase activity, which nevertheless induces a robust secretion of PCI. Thrombin formation by the prothrombinase complex was profoundly enhanced when the PCI-mediated PE transfer into the platelets was operating (Fig. 1 E). In contrast, PCI failed to increase the thrombin generation when the lipid donors were devoid of PE. Control experiments verified that no prothrombinase activity was elicited by the PE vesicles in the absence of the platelets (unpublished data). The anti-PCI antibody abrogated the thrombin formation, which indicates that the secreted PCI is a responsible factor (Fig. 1 E). Additional PCI further promoted the thrombin formation in the presence of the PE-containing donors but not with pure PC vesicles (Fig. 1 E). Our findings characterize PCI as a selective lipid transporter for PE that supports the cellular import of this phospholipid.

Rapid plasma membrane translocation and nuclear targeting of PCI

When visualizing the interaction of biotin-PCI with live HL-60 cells, we found that several cells rapidly incorporated the protein. After 10 min, PCI accumulated in the submembraneous region (Fig. 2 A). Heparin cofactor II (HC-II), a serpin with sequence similarity to PCI, was not incorporated (see Fig. 5 C; not depicted). After longer incubation times, PCI was increasingly targeted to the nucleus. We indeed observed accumulation of PCI in the perinuclear space and intranuclear compartments by immuno EM (Fig. 2 B). Time-dependent accumulation of PCI was also seen in isolated cytosolic and nuclear fractions (Fig. S2, available at http://www.jcb.org/cgi/content/full/jcb.200707165/DC1). The nuclear targeting of PCI might be facilitated by its H helix, because GFP-linked variants of PCI lacking the basic amino acids of this helix failed to enter the nucleus (unpublished data).

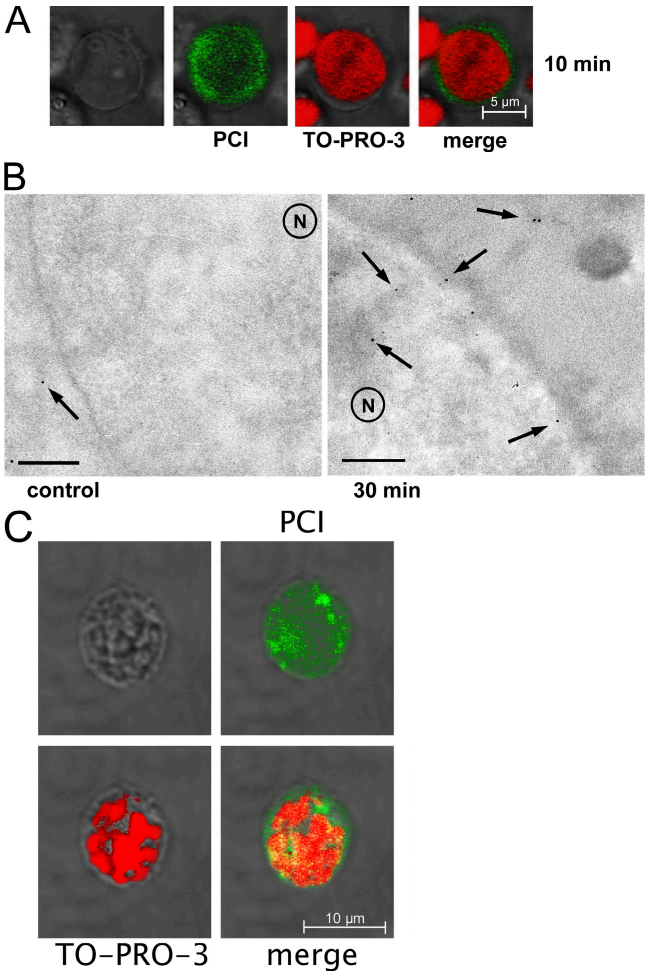

Figure 2. **Rapid cell entry and nuclear targeting of PCI.** (A) Internalization of PCI into live cells. Leukocytic HL-60 cells were incubated for 10 min with 90 nM of biotin-labeled uPCI (green) at 37°C, and intracellular staining of PCI was monitored by confocal microscopy at a focal plane allowing visualization of nuclei. Cell nuclei were stained with TO-PRO-3 (red). The images are representative of five independent experiments. (B) Intracellular PCI is directed to intranuclear compartments. Immunoelectron micrographs of HL-60 cells incubated with 90 nM of biotin-labeled rPCI for 0 (control, immediately processed for the analyses) and 30 min at 37°C. Arrows indicate PCI detected by gold-labeled anti-biotin antibody. No nuclear labeling of PCI is seen under control conditions. After 30 min of incubation, the serpin accumulates in the nucleus (N). Bars, 0.5 µm. (C) PCI is targeted to leukocyte nuclei in vivo. Biotin-labeled uPCI injected into the murine blood circulation is recovered within 30 min in the nuclei of granulocytes. Co-labeling of biotin-PCI with TO-PRO-3 in live granulocytes documents the nuclear localization of the serpin.

To explore whether the fast cell entry and nuclear targeting of the serpin was also operating in the intact organism, we injected biotin-labeled PCI into the tail vein of mice. The protein was allowed to circulate for 30 min in the vascular system. Thereafter, the total pool of leukocytes was prepared from the murine blood and cells were visualized by confocal microscopy. Thereby substantial costaining of PCI with the nuclear marker was noted in the granulocyte fractions (Fig. 2 C), which indicates that the protein had been integrated into the nuclei. We thus conclude that the cell entrance of PCI enables its rapid targeting to intranuclear compartments both in vivo and in vitro.

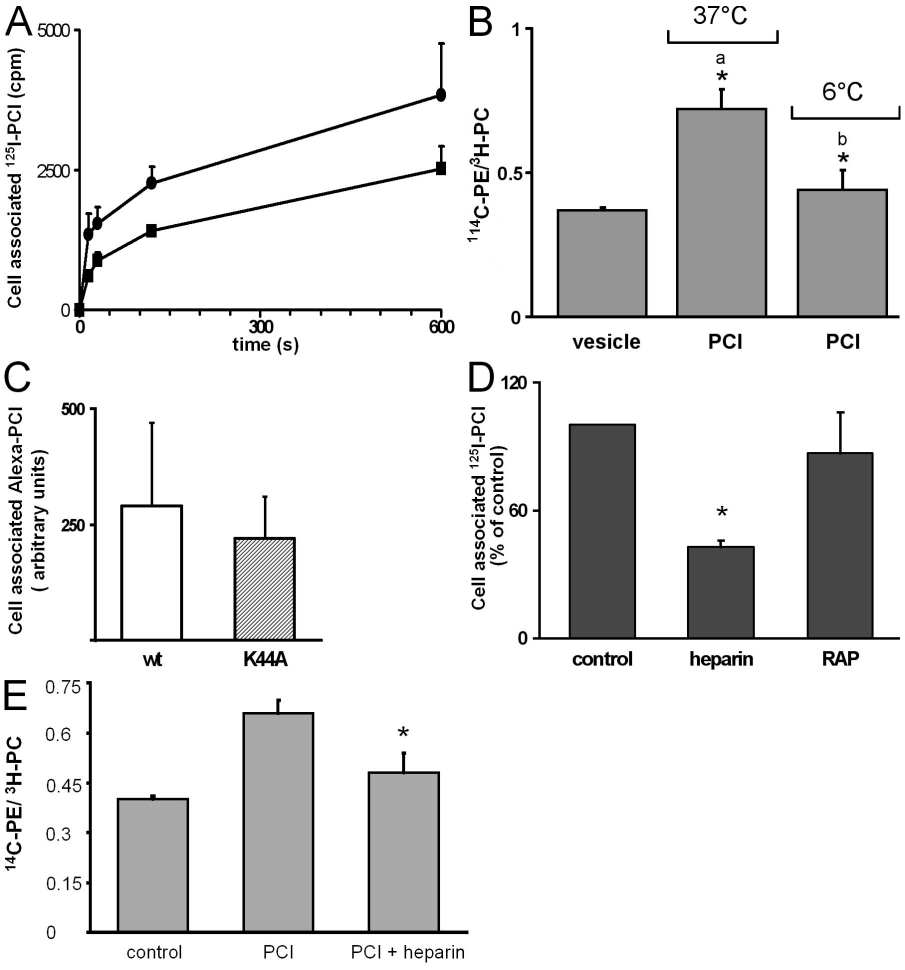

Figure 3. **Internalization of PCI is largely independent from temperature.** (A) Restricted temperature dependence of the cell entrance of PCI. Uptake of 20 nM of ^{125}I-labeled uPCI (^{125}I-PCI) by neutrophils was assessed at 37 (●) or 6°C (■). $n = 3–5$. (B) PCI fails to promote the cellular import of PE at 6°C. Neutrophils were incubated for 10 min with SUV (95 mol% PC and 5 mol% PE containing [^{14}C]PE and [^{3}H]PC) at the two indicated temperatures. vesicle, [^{14}C]PE/[^{3}H]PC ratio in the absence of uPCI. $n = 4$. *, $P < 0.05$ versus vesicle (a) or PCI at 37°C (b). (C) PCI internalization is mostly conserved in cells with disrupted dynamin2 function. Incorporation of Alexa 488–conjugated rPCI into CHO cells transfected with the dynamin2 K44A variant (or with wild-type dynamin2) was quantified at 37°C. $n = 4$. (D) Heparin inhibits PCI internalization. Neutrophils were incubated for 10 min at 37°C with 20 nM [^{125}I]PCI. Interaction with the glycosaminoglycans was prevented by 100 μg/ml heparin. Receptor-associated protein (RAP) was present at 0.4 μM. $n = 4$. *, $P < 0.05$ versus control. (E) Lipid transfer activity of PCI is decreased by heparin. Neutrophils were incubated with SUV containing [^{14}C]PE and [^{3}H]PC under conditions as in B. $n = 3$. *, $P < 0.05$ versus PCI alone. Results show mean ± SD.

To quantify the cellular internalization of PCI, neutrophils were first exposed to [^{125}I]PCI followed by the addition of a ligand dissociation buffer to exhaustively remove any proteins bound to the extracellular surface (Liu et al., 2000). Within the first 2 min of incubation at 37°C, a large proportion of PCI accumulated within the cells (Fig. 3 A). The incorporation then proceeded at a slower rate. The quantity of PCI internalized at 6°C amounted to 2/3 of the uptake at 37°C (Fig. 3 A). In contrast to the PCI internalization, the PE transferase activity of PCI was clearly diminished at low temperatures. Indeed, PCI failed to increase the [^{14}C]PE/[^{3}H]PC ratio at 6°C (Fig. 3 B). To further address the participation of endocytic routes, CHO cells were transfected with the K44A mutant of dynamin2 (Altschuler et al., 1998), which prevents the budding of vesicles necessary for internalization of cargo via several major endocytic routes. Intrusion of Alexa 488–PCI into K44A-transfected cells was only slightly lowered compared with the uptake observed in the wild-type cells (Fig. 3 C). Also, transfection with the AP180 variant AP180-C selectively repressing the clathrin-mediated pathway barely reduced PCI incorporation (unpublished data). A major proportion of PCI incorporation thus persists under conditions suppressing the classic endocytic pathways. Inclusion of heparin into the cell suspensions to prevent interaction of PCI with the cell surface (Priglinger et al., 1994) substantially lowered the cell entry of PCI (Fig. 3 D). In contrast, the internalization was largely unaffected by receptor-associated protein, which blocks the function of the low-density lipoprotein receptor–related protein (LRP/α_2 macroglobulin receptor), a mediator of the uptake of Tat (Liu et al., 2000). Heparin also abrogated the PCI-mediated cellular import of [^{14}C]PE, as is evident from its ability to prevent the PCI-elicited increase of the [^{14}C]PE/[^{3}H]PC ratio (Fig. 3 E).

PE essentially supports the internalization of PCI

To evaluate the contribution of PE for the cell entrance of PCI, the cells were preincubated with duramycin, a cyclic peptide that specifically interacts with this phospholipid (Navarro et al., 1985; Iwamoto et al., 2007). Duramycin dose dependently suppressed incorporation of PCI at 37°C (Fig. 4 A). The peptide also diminished cell entry of PCI at 6°C (Fig. S3 A, available at http://www.jcb.org/cgi/content/full/jcb.200707165/DC1), suggesting that the pathway supporting PCI internalization was still functioning at this temperature. Then, before the addition of duramycin, cell surface proteins were excessively cleaved by trypsin/proteinase K. Even so, the capacity of the PE-binding peptide to abrogate the PCI incorporation was maintained (Fig. S3 B). Although PE is a regular component of the external leaflet of the cell membrane (Zwaal and Schroit, 1997), its cell surface content increases under conditions of PS exposure. PCI can interact

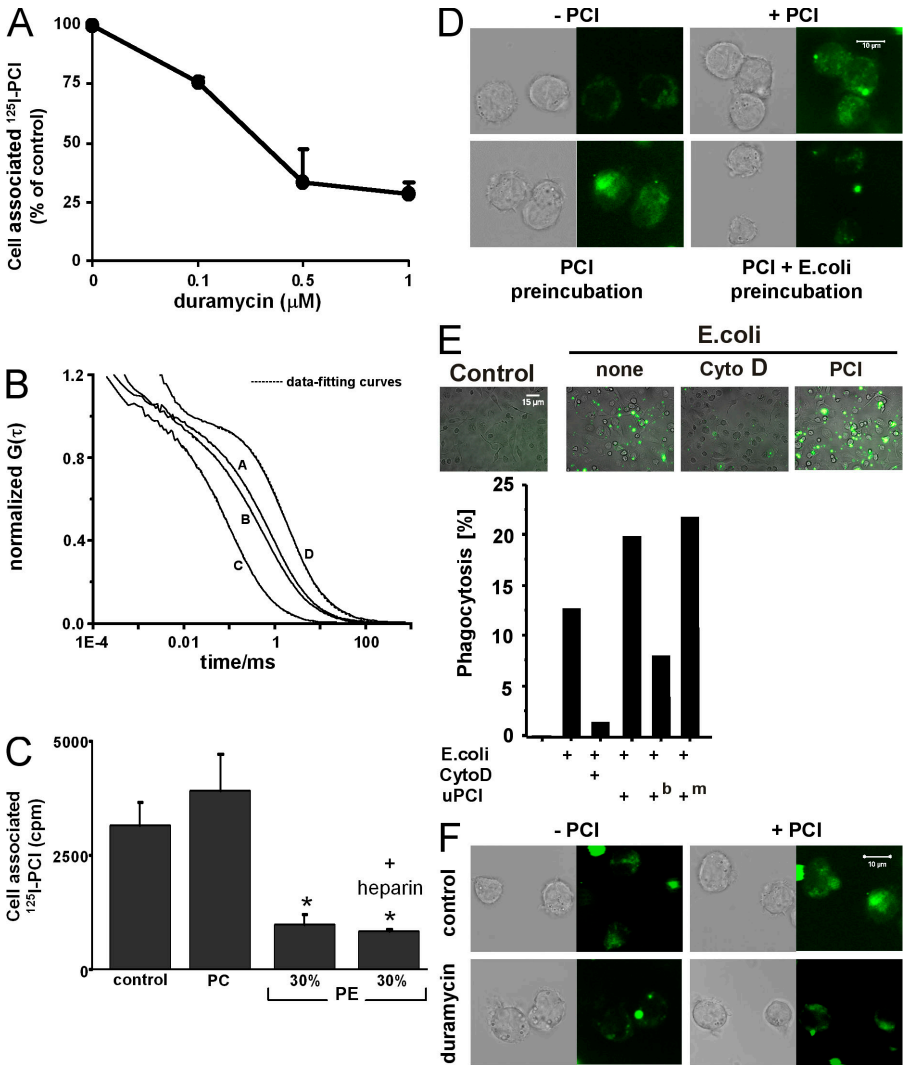

Figure 4. **Essential role of PE for the cellular internalization of PCI.** (A) Cell entrance of PCI is abrogated by duramycin. Concentration dependence of the inhibition of neutrophil [^{125}I]PCI uptake (10 min, 37°C) by duramycin. Results show mean ± SD. n = 3–5. (B) PE increases membrane association of PCI in the presence of PS. Autocorrelation curves from fluorescence correlation spectroscopy measurements, representing the diffusion of Alexa 488–uPCI in proximity to membranes of GUV composed of 30:65:5% PE/PC/PS (A) and 95:5% PC/PS (B). Curves C and D denote the diffusion of PCI in aqueous solution and of the hydrophobic probe DiD-C_{18} (D). Curves A and B could be fitted by diffusion coefficients corresponding to the protein diffusion in the membrane environment and the aqueous solution. The shift to the right indicates that more PCI molecules are membrane associated in the case of PE-containing vesicles. The data are representative of seven experiments. (C) Extracellular PE inhibits the cell entry of [^{125}I]PCI. SUV containing 100% PC or 30% PE and 70% PC were included into the neutrophil suspensions. Results show mean values ± SD. n = 4–6. *, $P < 0.05$ versus PC. (D) PCI enhances cellular uptake of *E. coli*. uPCI and FITC-labeled *E. coli* were incubated with live THP-1 macrophages. In other samples, the cells were preincubated for 30 min before the addition of bacteria or with the bacteria before addition of cells. The confocal microscopy pictures show mostly intracellular bacteria. The images are representative of three independent experiments. (E) Quantification of increased phagocytosis via PCI. (top) Representative experiment showing the uptake of FITC-labeled *E. coli* as quantified by flow cytometry. Where indicated, the cells were selectively preincubated with PCI, washed, and further incubated with bacteria. Inhibition by cytochalasin D (CytoD) indicates that uptake of *E. coli* occursby phagocytosis. (bottom) Phagocytosis is displayed as a percentage of FITC-positive macrophages (mean values of duplicates). b and m, PCI preincubated with bacteria and macrophages, respectively. (F) Stimulation of phagocytosis requires PCI–PE interaction. THP-1 macrophages were preincubated with or without uPCI in the absence or presence of 0.5 μM duramycin. The cells were washed once and FITC-labeled *E. coli* was added. The intracellular localization of the bacteria was visualized by confocal microscopy. The images are representative of three independent experiments.

with both aminophospholipids (Malleier et al., 2007). To specify the interaction of PCI with PE in the presence of PS, we used fluorescence correlation spectroscopy to calculate the diffusion coefficients of PCI bound to lipid vesicles and for free PCI (Fig. 4 B). The ratio of bound/free PCI amounted to 2.9 ± 0.2 in the case of the PE/PC/PS vesicles, whereas it was 1.5 ± 0.1 for the PC/PS vesicles (mean ± SD), indicating that the preferential interaction of PCI with PE persists in the presence of PS. To further evaluate the participation of PE for the internalization of PCI, we added lipid vesicles enriched with high concentrations of PE. This decreased the PCI internalization to an appreciable extent (Fig. 4 C). Cell entry of the serpin remained unchanged, with vesicles containing exclusively PC. In the presence of extracellular PE, heparin was unable to further diminish the protein incorporation (Fig. 4 C). The latter finding establishes that heparin and extracellular PE abrogate the same route of PCI internalization. PCI thus elementarily necessitates PE for its passage through the cell membrane.

PCI is expressed in several body cavities (Geiger, 2007) and hence macrophages poised to clear invading microorganisms from these compartments are continuously exposed to the serpin. Resting macrophages exhibit increased aminophospholipid exposure, which is enhanced during phagocytosis (Marguet et al., 1999). We found that the rapid internalization of PCI by THP-1 macrophages (unpublished data) was associated with an increased phagocytosis of *Escherichia coli* (Fig. 4 D). The effect was preserved when the phagocytes were first allowed to incorporate PCI and then exposed to the bacteria. In contrast, preincubation of the bacteria with PCI before the addition of THP-1 cells reduced phagocytosis. PCI stimulated phagocytosis of *E. coli* in cells in which the incorporation of the serpin was restricted to extranuclear regions of the cells, suggesting that the nuclear localization of PCI is not required for its ability to increase phagocytosis. Quantification by flow cytometry confirmed that PCI fosters the cell entry of bacteria (Fig. 4 E). Stimulation of phagocytosis was almost identical when PCI was removed

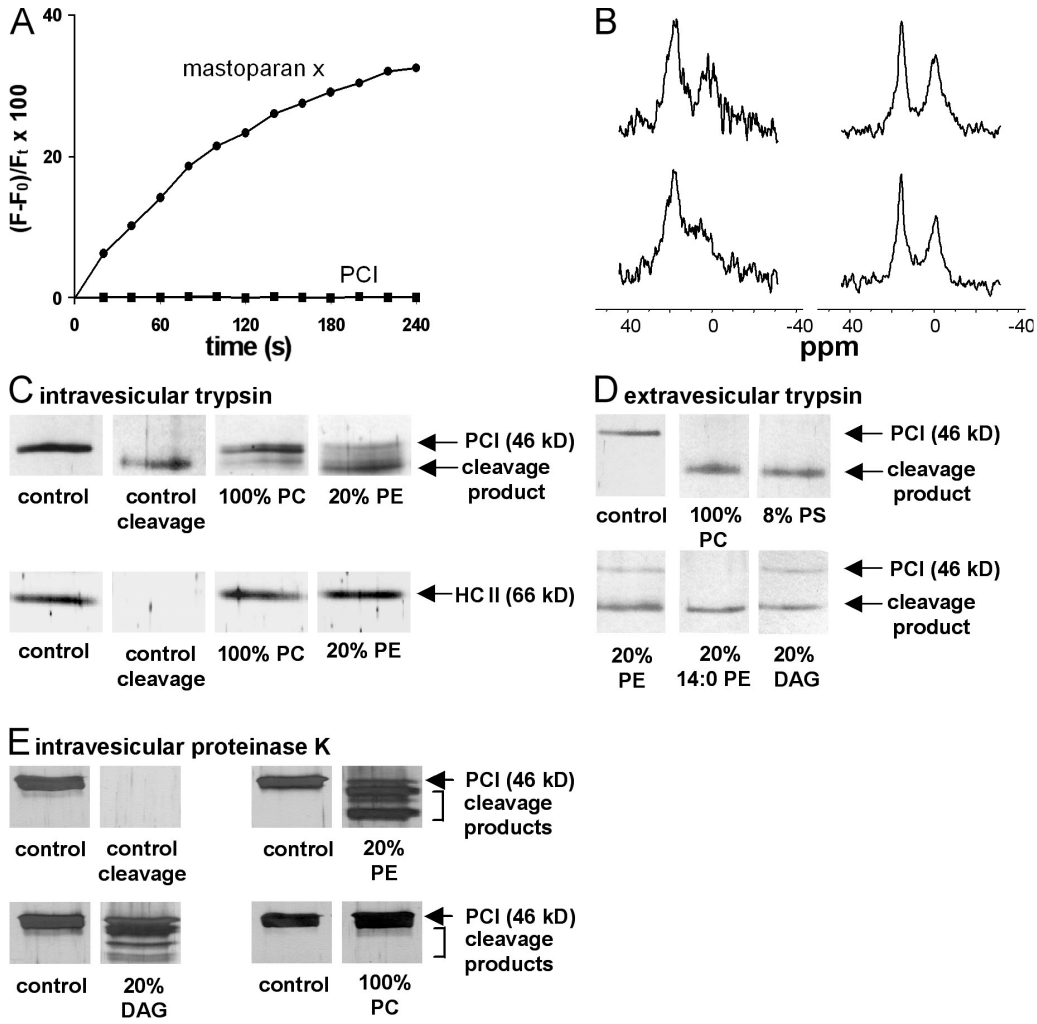

Figure 5. **PCI translocation is facilitated by cone-shaped lipids supporting formation of intramembrane aqueous compartments.** (A) PCI does not cause pore formation in membranes. CF was included in the aqueous core of LUV (30:70% PE/PC), and, subsequently, 0.5 μM rPCI or 4 μM mastoparan X (positive control) was added. Mastoparan X, but not PCI, induces the CF release. (B) PCI enables slow membrane translocation of a small hydrophilic molecule. ^{31}P-NMR spectra were recorded 300 min after addition of 5.7 mM Pr^{3+} and 40 nM uPCI (C and D) to the vesicle suspensions. (A and C) LUV with 30:70% PE/PC. (B and D) 100% PC. The decrease in intensity caused by line broadening of the phosphorous signal from the inner leaflet at 3 ppm (C) indicates cation influx into the vesicles. (C) Membrane partitioning of PCI. (top) 20 nM rPCI is accessible to intravesicular 0.5 mg/ml trypsin (37°C) in LUV containing long chain PE but not in pure PC vesicles. (bottom) Under the same conditions, HC-II remains uncleaved. (D) Cone-type lipids enforce membrane penetration of PCI. LUV were prepared from the indicated lipids, the vesicle matrix being PC (adding up to 100 mol%). After incubation with rPCI, 0.5 μg/ml trypsin was added. Part of the PCI remains unfragmented when the vesicles contain long chain PE and DAG but not with short chain PE or PS. (E) PCI reaches the aqueous core of lipid vesicles. Proteinase K in LUV supplemented with PE and DAG affords complete degradation of rPCI, indicating its protrusion into the vesicle interior. Conversely, the integrity of the protein is fully preserved in pure PC-LUV. Control cleavage (absence of vesicles) reveals complete PCI degradation (all cleavage products <15 kD). All protease experiments were repeated at least once.

after preincubation, whereas preincubation of PCI with bacteria suppressed their uptake (Fig. 4 E). This shows that stimulation of phagocytosis by PCI requires a direct interaction of the serpin with the cell membrane. Pretreatment of the macrophages with PCI in the presence of duramycin, which also inhibited PCI internalization into THP-1 cells (not depicted), decreased cell entry of *E. coli* (Fig. 4 F). In contrast, basal uptake of bacteria (absence of PCI) was unaffected by duramycin (Fig. 4 F). Hence, the specific membrane partitioning of PCI facilitates bacterial phagocytosis.

Membrane insertion of PCI is facilitated by cone-type lipids

Because several of the translocating peptides were previously shown to generate transmembrane pores (magainin-2 and mastoparan X; Matsuzaki et al., 1995; Schwarz and Arbuzova, 1995), we investigated whether PCI elicited pore formation. As a positive control, the peptide mastoparan X rapidly evoked nucleation of pores in large unilamellar vesicles (LUV; Fig. 5 A), as was evident from the leakage of intravesicular carboxyfluorescein (CF). In contrast, PCI did not elicit the formation of leakage sites for CF (Fig. 5 A), even after prolonged incubation (up to 120 min; not depicted). To evaluate whether PCI altered the membrane barrier properties for a small hydrophilic molecule, we monitored the membrane passage of the cation praseodymium (Pr^{3+}; Sillerud and Barnett, 1982). By using ^{31}P nuclear magnetic resonance (NMR), two peaks originating from the phosphate groups of the outer and inner monolayer phospholipids could be discerned (Fig. 5 B). In LUV containing solely

PC, the peak pattern was unchanged by prolonged incubation with the cation. However, the addition of PCI markedly reduced the height and broadened the peak representing the inner leaflet phospholipids when long chain PE was present (Fig. 5 B). This demonstrates a direct interaction of Pr^{3+} with the inner monolayer phospholipids. As a negative control, no changes in the inner monolayer peak were seen without PCI. PCI thus generates transient and subtle changes in the bilayer structure that result in the formation of an aqueous pathway within the membrane.

To evaluate whether PCI itself is inserted into the membrane, we added trypsin into the vesicle core. Whereas the serpin remained largely uncleaved by the intravesicular protease in pure PC vesicles, it was clearly degraded when the membrane contained long chain (unsaturated) PE (Fig. 5 C). In contrast to PCI, the integrity of HC-II was fully conserved in the presence of the intravesicular trypsin, irrespective of the lipid composition of the vesicles (Fig. 5 C). In a complementary procedure, PCI was first incubated with the lipid vesicles and subsequently treated with extravesicular trypsin. In the presence of PE, part of the PCI remained refractory toward cleavage by the extravesicular trypsin (Fig. 5 D). In contrast, PCI was completely degraded in suspensions of the pure PC and PC/PS vesicles. The ability of PCI to penetrate into the bilayer thus crucially requires PE.

Partitioning of PCI into the lipid bilayer could be facilitated by a specific binding to PE (e.g., via interactions with the ethanolamine head group) and/or changes in the physicochemical properties of the membrane. In the latter case, nonbilayer domains, which are particularly favored by the conical shape of PE, could be involved (Israelachvili, 1980; de Kruijff, 1997). When the LUV were prepared from a short chain species of PE with a cylindrical morphology (di-14:0-PE), the protein was entirely degraded by extravesicular trypsin, similar to the findings obtained with the pure PC vesicles (Fig. 5 D). However, in LUV consisting of a lipid with a conical configuration but devoid of the ethanolamine head group DAG, PCI was partially resistant toward cleavage by the protease (Fig. 5 D). This suggests that the conical shape of long chain PE is essential for the membrane penetration of PCI. To further substantiate the extent of membrane insertion of the serpin, we exploited the ability of proteinase K to excessively degrade the serpin (Fig. 5 E). When the protease was integrated into the aqueous core of vesicles containing long chain PE, PCI was cleaved into several high molecular mass degradation products (Fig. 5 E), confirming that PCI protrudes into the vesicle core. In LUV supplemented with DAG, very similar fragmentation products were apparent. Conversely, after inclusion of the protease into vesicles only consisting of PC, the integrity of the protein was fully conserved (Fig. 4 E). This confirms that the serpin failed to reach the vesicle core in the presence of PC alone. Overall, our findings suggest that the conical shape of long chain PE is essential for the membrane penetration of PCI, which adopts a location that completely spans the bilayer.

PCI translocation requires key components of the hydrophobic pocket allowing selectivity of lipid interaction

Molecular docking studies based on the crystallographic structure of PCI (Huntington et al., 2003) were undertaken to characterize the structural components of PCI enabling its distinctive interaction with phospholipids. In view of the flexibility of the entire PE molecule, we chose a rigid fragment of the saturated hydrocarbon chain (C11 fragment) for the initial docking analysis because saturated fatty acyl chains are esterified to the C1 atom of the glycerol backbone of (diacyl-)PE under biological conditions (Fig. S4, available at http://www.jcb.org/cgi/content/full/jcb.200707165/DC1). Docking of the C11 fragment onto the PCI structure revealed 276 clusters with energies (kJ/mol) better than −15 among a total of 25,242,070 calculations. The two best clusters were nearly identical in position and energy (both better than −28 kJ/mol) and were significantly separated from the other clusters, with the next best hit at −24.3 kJ/mol. The best-docked C11 fragment fit into a capped hydrophobic pocket along helix D (D′ channel; Fig. 6 A). The orientation of the saturated chain was thus fixed. Consequently, the possible positions of the unsaturated chain, canonically esterified to the C2 atom of PE, were spatially limited to the same region. Of the top 10 clusters, two provided a portion of the possible binding site for the unsaturated hydrocarbon chain (9th and 10th best energies). It was found to be best accommodated by a second hydrophobic channel running along helix H (H′ channel), in close proximity to the PCI-binding site for heparin (Figs. 6 A and S4, helix H). Moreover, in view of the locations revealed for the acyl chains, the position of the head group of PE was also suggested. The entire PE molecule was built on the two hydrocarbon chains placed by the docking studies and subjected to energy minimization. In the final model (Fig. 6 A), the ethanolamine group is found to be located in close proximity to Leu78, whereby the formation of an H bond between the N atom of the ethanolamine group and the main chain oxygen of Leu78 could be enabled. Space limitations within this region principally impair the interaction of PCI with phospholipids containing larger head groups than PE such as PC.

To explore the role of the hydrophobic pocket for the PE-dependent membrane insertion of the serpin, PCI residues potentially implicated in the lipid binding were mutated. L78 was substituted by Trp to prevent the proposed interaction of the protein with the ethanolamine head group. Consequently, the variant remained completely undigested in the presence of the intravesicular proteinase K, oppositely to the native protein (Fig. 6 B). Substitution of V374, a component of the H′ channel suggested to mediate the binding of the sn-2 fatty acyl chain of PE, by Trp also conferred resistance toward cleavage by the intravesicular protease (Fig. 6 B). Both amino acid exchanges thus suppress the ability of PCI to partition into the vesicle core. In contrast, mutations of residues R35 and T341, both being unrelated to the proposed lipid binding site, did not perturb the PCI penetration into the vesicle center (unpublished data). A qualitatively different digestion pattern was noted when three Ala were inserted at position 376 (Fig. 6 B). This insertion was implemented to restitute the loop between the last two β strands specifically truncated in PCI while attenuating its hydrophilic properties. Part of the PCI species was accessible by the intravesicular enzyme, as was evident by the appearance of digestion products (Fig. 6 B), arguing for its protrusion into the vesicle core. To further detail the extent of membrane penetration, the

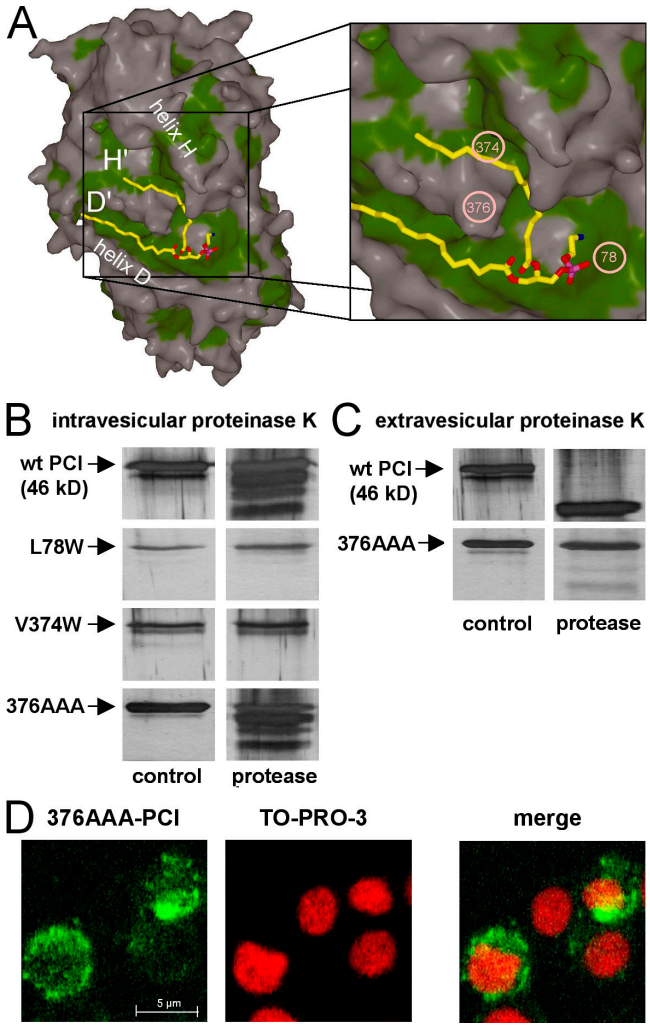

Figure 6. **Hydrophobic cavity accommodating PE drives protein translocation.** (A) Energy-minimized model of PE bound to PCI. The model is based on the two hydrocarbon docking solutions shown in Fig. S4 (available at http://www.jcb.org/cgi/content/full/jcb.200707165/DC1). The positions of the H and D helices are indicated as are the channels after which they are named. The close up demonstrates the suitability of this feature of PCI for binding to diacyl phospholipids. Moreover, the positions of the amino acids are indicated subjected to mutagenesis in B–D. Green indicates hydrophobic areas of the protein. (B) Amino acid substitutions of the proposed lipid binding site impair PCI translocation. Native and mutagenized PCI species (20 nM) were incubated with PE vesicles containing intravesicular proteinase K. Contrary to the native protein, mutations in the head group and fatty acid–binding regions (L78W and T374W) prevent the protein from degradading, indicating incomplete incorporation into the bilayer. The 376AAA insertion mutant is strongly digested, which suggests its full penetration into the bilayer. (C) 376AAA insertion enhances membrane intrusion of PCI. In the presence of extravesicular proteinase K, the full-length form of native PCI is completely lost. In contrast, the 376AAA insertion is resistant to fragmentation by the protease, confirming the disappearance of the variant from the extravesicular compartment. (D) PCI variant 376AAA is rapidly directed to intranuclear compartments. HL-60 cells were incubated for 10 min with 90 nM of the biotin-labeled PCI variant (green) at 37°C and analyzed by confocal microscopy. In parallel, cell nuclei were stained with TO-PRO-3 (red).

variant was exposed to extravesicular proteinase K. Thereby, the mutant remained almost entirely refractory toward proteolytic attack (Fig. 6 C). In contrast, under the same conditions, the complete loss of the substrate and limited cleavage into a single high molecular mass degradation product was noted for the native protein (Fig. 6 C). The differential digestion pattern for the wild-type PCI in the presence of the intra- versus extravesicular protease (Fig. 6, B and C) excluded a passage of the enzyme across the bilayer. The findings thus suggest that the 376AAA insertion strongly facilitates the membrane translocation of PCI. This conclusion was enforced by experiments with intact cells. After a 10-min incubation period, the labeled 376AAA variant was found to be rapidly internalized by HL-60 cells (Fig. 6 D). In particular, during the short exposure, a noticeable proportion of the mutant was incorporated into the nucleus (Fig. 6 D), in contrast to what had been observed with the native serpin (Fig. 2 A). Overall, the findings establish that the branched hydrophobic cavity in between helices H and D is of basic importance for the membrane insertion and transmigration of PCI.

Discussion

We demonstrate that the internalization of a new cell-penetrating protein, the serpin PCI, is essentially supported by the plasma membrane lipid PE. Lipids are known to contribute to the interaction and insertion of proteins into intracellular and bacterial membranes (van Klompenburg et al., 1998; Kuwana et al., 2002). However, their contribution to the protein insertion into the plasma membrane and consequently the protein internalization into cells is less well documented. Our findings now reveal that cell surface–exposed PE is a major mediator of the protein translocation across the plasma membrane. The essential contribution of PE is corroborated by the ability of the PE-binding peptide duramycin to abrogate protein uptake, the failure of the serpin to cross the cell membrane in the presence of extracellular PE, and the selective PE requirement for membrane penetration of PCI. Interaction of PCI with PE is preceded by docking of the serpin to negatively charged surface molecules such as glycosaminoglycans. This suggests that two basic steps, initial cell surface docking and subsequent interactions with PE, mediate the membrane insertion and cell entry of the protein. Importantly, we show that the distinct conical shape of PE (Israelachvili et al., 1980; de Kruijff, 1997) represents a major driving force for the membrane translocation of PCI.

PE is the eminent plasma membrane lipid with a cone-type morphology because the concentrations of similarly shaped lipids (DAG and phosphatidic acid) are considerably lower. Mechanistically, DAG also efficiently supported the membrane penetration of PCI, whereas the protein intrusion was prevented by cylindrical PE species. This suggests that the conical shape of PE is of greater relevance for the interaction with PCI than specific interactions with the ethanolamine head group. Despite the bilayer-spanning location of PCI, the protein was not entirely transferred to the vesicle core, suggesting that its incorporation into the cell interior requires additional membrane components. Moreover, although transmembrane pores were not implicated in the PCI translocation, which is consistent with the inability of the conical lipids to support the pore formation (Matsuzaki et al., 1998), the serpin was found to elicit subtle perturbations of the membrane organization, as indicated by the leakage of ions from the lipid vesicles. This indicates that the PCI–PE interaction induces the formation of aqueous compartments within the membrane.

Lipids of cone-type morphology are principally capable of generating areas of negative curvature in membranes (Farsad and De Camilli, 2003). This can facilitate the formation of intramembrane nonbilayer domains (inverted micelles), which might assist in the formation of aqueous compartments within the membrane. At present, it is unclear how the PCI–PE interaction mediated by the docking of the lipid to a distinct hydrophobic groove in PCI in the molecular system (see last paragraph of Discussion) relates to the alterations in physicochemical properties by the cone-shaped lipids that allow PCI transfer across the membrane. Hence, more in-depth analyses will be required in future studies to clarify whether these two observations are indeed interrelated. Overall, our results indicate that the membrane passage of PCI is crucially driven by lipids of a distinct morphology that generate an aqueous translocation route for the protein via the generation of nonbilayer domains.

The lipid-dependent internalization of cell-penetrating PCI principally agrees with a model theoretically proposed for the internalization of the translocating peptides (Joliot and Prochiantz, 2004). However, a contribution of PE and its peculiar shape for the cellular uptake of proteins has never been revealed. Cone-shaped lipids faciliate membrane fusion and budding processes (McMahon and Gallop, 2005), which are required for the formation of phagosomes. Consequently, the enhancement of bacterial phagocytosis induced by the PCI–PE interaction as observed here could be enabled by the stimulation of phagosome maturation. The ability of PCI to foster removal of pathogens suggests its participation in host defense and thus overlaps with the functions of other cell-penetrating proteins implicated in innate immunity. The internalized PCI was found to be rapidly directed to the nucleus, both in vitro and in the intact organism. Our findings position PCI as a promising candidate for the rapid delivery of cargo to the nucleus, including viruses, nucleotides of differing length and structures, and proteins/peptides. Being a component of the human proteome, potential applications of cargo-loaded PCI in humans are not immunogenic. PCI might be exploited in particular for the targeting of cargo into cells with increased surface exposure of PE (Vance, 2003), including capacitated sperm (Gadella and Harrison, 2000) and others.

PCI is shown to selectively extract PE from lipid particles, consecutively inserting the lipid into the plasma membrane of various cells. PCI thus belongs to a new class of proteins promoting the cellular uptake of selective lipids, including those specific for phosphatidylinositol (Wang and Munford, 1999) and sphingoymyelin (Stoeckelhuber et al., 2000). The latter proteins do not share structural homologies with PCI, a situation known from the intracellular lipid transfer proteins (Wirtz, 1997). During the transfer, the phospholipid would have to be largely protected from the contact with water, as revealed for scavenger receptor class B type I, the prototype mediator of the cellular phospholipid import (Urban et al., 2000). Based on the velocity, extent, and temperature dependence of the PE import, we assume that a principally similar process allows PCI to ferry PE into the cells. Only a limited change in the conformation of the protein–lipid complex might be required to switch between the extra- and intramembrane modes of the PCI–PE interaction. Indeed, the protein is most likely integrated into aqueous compartments during the membrane translocation. Nonetheless, at low temperatures, the lipid transferase activity of PCI is suppressed, whereas the PE-dependent PCI internalization is largely maintained. This indicates that the PE transfer is energy independent, whereas the membrane translocation of PCI exhibits a limited energy requirement, a property common to several cell-penetrating proteins. Whereas PCI facilitates PE enrichment on the cell surface by virtue of its lipid transferase activity, PE accumulation is further assisted by the delayed transbilayer movement of the lipid (Morrot et al., 1989). We observe that PE insertion accelerates the activity of the prothrombinase complex, thereby amplifying the formation of thrombin, a major coordinator of blood coagulation. Once internalized, PCI could potentially also support the intracellular movement of PE, such as between the cell membrane and membranes of intracellular organelles. Overall, our findings characterize PCI as the first transferase specifically fostering the cell import of PE.

Using the crystal structure of PCI as a template, we revealed that the selective interaction of PCI with PE is facilitated by a dual-channelled hydrophobic groove that is generated by the shortened A helix and a truncated loop between strands 3 and 4B. The H′ and D′ channels arising therefrom accommodate the extensions of the fatty acyl chains of the phospholipid with sharp precision. Indeed, because the H′ channel is not capped, it can house hydrocarbon chains of up to 22 C atoms, the longest unsaturated fatty acids esterified to PE in mammals. Moreover, the restricted size of the structure in which the phospholipid headgroup is buried markedly favors interactions with conical phospholipids. Hydrogen bonds between the ethanolamine group and specific amino acids, suggested to permit the folding of bacterial lactose permease (Bogdanov et al., 1999), might additionally ease the interaction with the phospholipid, as exemplified by the functional contribution of Leu78. Together, this structural constellation is supposed to enable the higher affinity of PCI for PE over PC. The docking and energy minimization studies were corroborated by the mutagenesis of single amino acids designed to specifically remodel the hydrophobic cavity. In particular, the insertion of a triple Ala sequence on top of the H′ channel substantially promoted the intrusion and membrane translocation of the serpin. The insertion, which reconstitutes the truncated loop intercalated between strands 3 and 4B, is likely to strengthen the interaction with the fatty acyl chains of the phospholipids by virtue of its specific location and enhanced hydrophobicity. In conclusion, the hydrophobic pocket appears to represent a unique structure for accommodating lipids capable of supporting the membrane passage of proteins.

Materials and methods

Cells

Human platelets were isolated from citrated blood as described previously (Engelmann et al., 1998). For isolation of neutrophils, the buffy coats from human blood anticoagulated with citrate were incubated with microbeads coupled to anti-CD15 antibodies for 15 min at 8°C. The suspensions were applied onto the positive selection column (Miltenyi Biotech) and the neutrophils were eluted with buffer. The purity of the neutrophil suspensions was >95% and the viability of the cells was 98% (trypan blue exclusion). CHO cells were transfected with pcDNA3 wild-type dynamin2 and its dominant-negative K44A mutant (provided by S. Egan, The Hospital for

Sick Children, Toronto, Canada). Cells were cultured in Iscove's modified Dulbecco's medium containing 20% FBS (HL-60) or DME supplemented with 10% FCS (CHO).

Preparation of native PCI and PCI variants

For preparation of recombinant PCI, the cDNA of human PCI was amplified from a human liver cDNA library using a forward (5′-CCGCTCGAGCATATG-CACCGCCACCACCCCCGGGAG-3′) and reversal primer (5′-CGGGATCC-ATCATCAGGGGCGGTTCACTTTGCCAAG-3′). Mutagenesis was performed using the QuickChange site-directed mutagenesis kit (Stratagene). The following mutants were generated: V374W, T341R, L78W, R35A, and 376AAA. All mutations were confirmed by DNA sequencing. After transformation of *E. coli* with the plasmids, 0.4 mM IPTG was added to induce the expression of the proteins. Bacterial supernatants were applied to a TALON Metal Affinity Resin column (Clontech Laboratories, Inc.) and the fractions eluted from the column were analyzed by SDS-PAGE. Urinary PCI (uPCI) was purified as described previously (Priglinger et al., 1994).

Phospholipid exchange

For the determination of the intervesicular phospholipid exchange, py-labeled donor vesicles and unlabeled acceptor vesicles were coincubated for different time periods, the suspensions were passed over an anion exchange column (Bio-Rad Laboratories), and the fluorescence was determined in Triton X-100 (Sigma-Aldrich) solubilisates of the acceptor vesicles as described previously (Stoeckelhuber et al., 2000). The vesicle preparations and incubations were performed in the presence of 10 nM butylated hydroxytoluene and under argon or nitrogen. The transfer of py-labeled phospholipids into the cells was analyzed as described previously (Urban et al., 2000). Under principally similar conditions, the cells were incubated with lipid donor vesicles containing traces of [^{14}C]PE (1-palmitoyl, 2-linoleoyl species) and [^{3}H]cholesterol (both from GE Healthcare).

Confocal microscopy

Washed HL-60 cells and murine leukocytes (see Incorporation of PCI…) were incubated with biotin-labeled PCI at 6 or 37°C. The cells were fixed with 4% paraformaldehyde for 60 min at room temperature, permeabilized with 0.1% Triton X-100 in 0.1% sodium citrate for 2 min at 4°C, and washed thereafter. Nonspecific binding sites were saturated overnight at 4°C with antibody dilution buffer (Dako) containing 0.2% goat serum. Subsequently, the cells were incubated for 60 min with Cy-2–labeled streptavidin (GE Healthcare) and an additional 30 min with TO-PRO-3 (Invitrogen). The cells were transferred onto slides and covered with Vectashield (Vector Laboratories). Slides were analyzed at room temperature with a laser scanning microscope (LSM 510 Meta; Carl Zeiss, Inc.) using a Plan-neofluar 40×, 1.3 oil differential interference contrast 1056–602 (1083–997) objective lens (Carl Zeiss, Inc.) and 488-nm Ar2 and 633-nm HeNe2 lasers. Images were obtained with a PMT photomultiplier tube (Hamamatsu Photonics). Image acquisition and processing was performed with LSM 510 image examiner software (Carl Zeiss, Inc.).

For analysis of phagocytosis of *E. coli* into THP-1 macrophages, the cells (10^5/well) were seeded in 24-well plates in 500 μl RPMI-1640 supplemented with 10% heat-inactivated FCS, 1% Hepes, 500 U/ml penicillin, and 500 μg/ml streptomycin and differentiated by the addition of 10 nM PMA. After 16 h, the cells were fed with fresh, PMA-free medium and cultivated for two more days. The macrophages were incubated with Alexa 488–labeled uPCI or FITC *E. coli* alone or together with their nonfluorescent counterparts in serum-free medium. Some samples were treated with duramycin (Sigma-Aldrich) for 15 min before the start of the incubations. The samples were visualized with a confocal laser scanning microscope (LSM 510 META). The images were taken by using a 63× Plan-Apochromat oil objective (Carl Zeiss, Inc.). Alexa 488 and FITC were irradiated at 488 nm and detected via a 505 longpass filter (Carl Zeiss, Inc.). The images obtained were analyzed and quantified using LSM Image Browser software (Carl Zeiss, Inc.).

Immuno EM

HL-60 cells previously incubated with or without 90 nM of biotin-labeled PCI were washed and fixed with 4% paraformaldehyde/5% glutaraldehyde for 60 min at room temperature. Before embedding in LR white medium resin (Pelco), the HL-60 cells were fixed with 2.5% glutaraldehyde in 0.1 M cacodylate buffer and then rinsed in 0.1 M phosphate buffer. Ultrathin serial sections of 150 nm were cut and mounted on gold grids. Nonspecific binding sites on the sections were blocked with 5% BSA in PBS, and grids were incubated for 120 min at 37°C with 10 nm of gold-labeled goat anti-biotin IgG (Biocell Laboratories, Inc.). The sections were then counterstained with 3% uranyl acetate and lead citrate and examined with a transmission electron microscope (JEM TEM 1200 EXII; JEOL Ltd.).

Incorporation of PCI by murine leukocytes in vivo

4 μg of biotin-labeled recombinant PCI (rPCI) was injected into the tail vein of anaesthetized mice. After 30 min, blood was drawn from the periorbital sinus into 0.38% sodium citrate, immediately diluted by 1:10 with erythrocyte lysis buffer (155 mM NH_4Cl, 10 mM $KHCO_3$, and 0.1 mM EDTA, pH 7.4), and centrifuged at 400 *g* for 20 min. The pellets were washed three times with decreasing volumes (1.5, 0.5, and 0.1 ml) of erythrocyte lysis buffer. The leukocytes obtained were processed for confocal microscopy as described previously.

Phagocytosis assay

THP-1 cells were differentiated with PMA as described in Confocal microscopy. Subsequently, the cells were washed in serum-free medium, mixed with 2×10^7 FITC-labeled *E. coli* (Vybrant Phagocytosis Assay kit; Invitrogen) in a final volume of 500 μl, and incubated for 2 h at 37°C in the presence or absence of 100 nM uPCI, 50 μM cytochalasin D, or 10% (vol/vol) human serum. In the preincubation experiments, either macrophages or bacteria were separately preincubated with 100 nM uPCI in serum-free medium for 60 min at 37°C and washed once before being added to the phagocytosis assay. After 2 h, noninternalized bacteria were rinsed away (after rinsing fluoroscence images were taken) and loosely attached *E. coli* were removed by trypsinization. The phagocytes were collected by centrifugation, resuspended in ice-cold PBS, and analyzed by flow cytometry (FACSCalibur; BD Biosciences).

Quantification of cellular internalization of PCI

uPCI was labeled with ^{125}I (GE Healthcare) by adding 100 μCi of the isotope to 50 μl of 0.25 M sodium phosphate buffer, pH 7.0, followed by the immediate mixing with 10 μl of 5 mg/ml chloramine T solution. 5 min after addition of 2.5 μg PCI, the reaction was stopped by inclusion of 50 μl of a saturated sodium ascorbate buffer, pH 7.0, and the labeled protein was purified from the unreacted ^{125}I via passage over a Sephadex-G10 column (GE Healthcare). After incubation with the labeled PCI, the cells were washed once with PBS and incubated for 30 min at 4°C with ligand-dissociation buffer (0.05% trypsin, 0.5 M EDTA, and 50 μg/ml proteinase K in PBS; Liu et al., 2000). The suspensions were centrifuged, the extracellular media were discarded, and the radioactivity of the pellets was determined. Alexa fluorescence intensity was measured in detergent-treated pellets (2% Triton X-100).

Prothrombinase activity

The activity of the prothrombinase complex was determined as described previously (Zieseniss et al., 2001).

Western blots

HL-60 cells were incubated with 100 nM PCI at 37°C, and the cell pellet was resuspended in nuclear extraction buffer 1 (10 mM Tris-HCl, 10 mM KCl, 0.5% IGEPAL CA-630, and protease inhibitor cocktail Complete; Roche), incubated for 30 min on ice, and lysed by sonication. The supernatants obtained from the homogenates were centrifuged and the resulting supernatants were used for separation of the cytosolic proteins. The pellets of the homogenates containing the nuclei were resuspended in extraction buffer 2 (10 mM Tris-HCl, 0.5M NaCl, and Complete), incubated for 30 min on ice, and centrifuged for 30 min, and the supernatants were recovered. After 10% SDS-PAGE, the proteins were transferred onto polyvinylidene fluoride membranes (Millipore), blocked overnight with 5% dry milk, and incubated for 60 min with anti-PCI antibody. After incubation for 45 min with horseradish peroxidase–conjugated anti–rabbit IgG, the proteins were visualized.

Translocation of PCI across pure lipid membranes

LUV were prepared from 10 mg of total lipids per milliliter in a buffer composed of 20 mM Hepes and 150 mM NaCl, pH 7.5, and supplemented with 0.5 mg/ml trypsin or 0.1 mg/ml proteinase K (intravesicular proteases). The various lipids (1-palmitoyl, 2-linoleoyl species of PC and PE, dimyristoyl-PE, dioleoyl-DAG, and PS) were dispersed by vortexing with glass beads. They were passed several times through an extruder (100 or 200 nm filters; LiposoFast; Avestin) until the solution was clear. The vesicle suspensions were subsequently dialyzed. Then the vesicle suspensions were incubated with PCI for 60 min at 37°C. The vesicle preparations and incubations were performed in the presence of 10 nM butylated hydroxytoluene under argon or nitrogen. Incubations with the intravesicular proteases

were performed in the presence of 2 mM of the protease inhibitor PMSF. Where indicated, the preparation of the LUV was performed before the proteases, and trypsin or proteinase K were added after the incubations with PCI (extravesicular proteases).

Efflux of CF from LUV

The lipids were dispersed in a buffer composed of 10 mM Hepes, 100 mM KCl, and 1 mM EDTA, pH 7.4, containing 60 mM CF (mixed isomers; Sigma-Aldrich). The vesicles were sized using 200-nm polycarbonate filters and separated from the extravesicular CF by dialysis. The fluorescence signal F was recorded after addition of mastoparan X and PCI at 37°C. In the case of pore formation, dequenching of the dye upon dilution into the medium will increase the values above the initial value F_o. To determine the fluorescence signal for the maximally releasable amount of CF (F_t), the vesicles were solubilized using the detergent $C_{12}E_8$.

Fluorescence correlation spectroscopy

Giant unilamellar vesicles (GUV) were prepared from 1-palmitoyl, 2-linoleoyl species of PC and PE together with 5 mol% dipalmitoyl-PS. For determination of the translational diffusion coefficient D_T, 10^{-4} mol% of DiD-C_{18} (Invitrogen) was added. The dispersed lipids were transferred to a coverglass chamber (Lab-Tek; Nalge Nunc), the formed GUV were allowed to settle for 20 min, and 9 nM Alexa 488–PCI was added. The fluorescence correlation spectroscopy measurements were performed in the autocorrelation mode with the ConfoCor 2 system (Carl Zeiss, Inc.) using either the 488-nm line of an Ar-ion Laser or a 633-nm HeNe Laser (at 50–60 μW). The excitation light was reflected by a dichroic mirror (HFT 488/633; Carl Zeiss, Inc.) and focused onto the sample. The emitted fluorescence light was split by a second dichroic mirror (NFT 635; Carl Zeiss, Inc.), passed through two filters (505–550 nm bandpass and 650 nm longpass filter; Carl Zeiss, Inc.), and detected in two separate channels. In each case, out of plane fluorescence was reduced by a pinhole of 90-μm diameter. For analysis of the membrane interaction of PCI, the fluorescence correlation spectroscopy focal spot was positioned near the center of the upper membrane of the GUV. For characterizing the diffusion properties of PCI in aqueous solution, the focus was moved to a position 20 μm above the upper membrane. The data were evaluated by Levenberg-Marquardt nonlinear least squares fitting to the appropriate model of the autocorrelation function.

Pr^{3+} transfer into vesicles

LUV of a diameter of 200 nm were prepared by the extrusion method (see Translocation of PCI…) and Pr^{3+} was added to a final concentration of 5.7 mM. The chemical shifts of the ^{31}P signals from the phospholipids present in the outer and inner leaflet of the LUV were registered. NMR spectra were recorded with a spectrometer (400S; Varian Medical Systems).

Docking studies

Based on the crystal structure of cleaved PCI (Huntington et al., 2003), docking studies for PE binding were performed with the program DockVision. Because of the extreme flexibility of the PE ligand, the docking studies were initially performed on a straight 11-carbon chain fragment (generated using CORINA; Huntington et al., 2003) meant to represent a possible conformation of the fully saturated hydrocarbon chain of PE. The maximum floating radius was set at 100 Å to ensure full coverage of PCI, and a total of 10,000 trials with a schedule of six conditions of 500 steps each was used in docking. The model of the PE–PCI complex using the 1-palmitoyl, 2-linoleoyl species of PE was built in XtalView (Huntington et al., 2003) and energy minimized using CNS (one cycle of 2,000 steps; Brunger et al., 1998).

Statistics

The mean values given are ± SD. The determinations were compared by one-way analysis of variance. Differences of $P < 0.05$ were considered to be significant.

Online supplemental material

Fig. S1 shows that inhibition of PCI decreases PE import into activated platelets. Fig. S2 indicates that uPCI added to HL-60 cells is incorporated into nuclear fractions of those cells. Fig. S3 shows that the PE-dependent internalization of PCI is also detected at low temperatures and under conditions of extensive proteolysis of cell surface proteins. Fig. S4 provides results from molecular docking analyses indicating the presumed PE binding site in PCI. Online supplemental material is available at http://www.jcb.org/cgi/content/full/jcb.200707165/DC1.

We would like to thank Stefan Nussberger for valuable suggestions as well as Markus Wiedmann and Christoph Reinhardt for help with the CF and PCI internalization experiments. We furthermore thank Jan Zaujec for his assistance in the mouse injection studies and Ingrid Jerabek for excellent technical assistance.

This study was supported by grants from the Deutsche Forschungsgemeinschaft to B. Engelmann and from the Austrian Science Foundation (projects P16093-B04 and P17337-B09) to M. Geiger.

Submitted: 24 July 2007
Accepted: 24 October 2007

References

Acton, S., A. Rigotti, K.T. Landschulz, S. Xu, H.H. Hobbs, and M. Krieger. 1996. Identification of scavenger receptor SR-BI as a high density lipoprotein receptor. *Science*. 271:518–520.

Altschuler, Y., S.M. Barbas, L.J. Terlecky, K. Tang, S. Hardy, K.E. Mostov, and S.L. Schmid. 1998. Redundant and distinct functions for dynamin-1 and dynamin-2 isoforms. *J. Cell Biol.* 143:1871–1881.

Bevers, E.M., P. Comfurius, D.W. Dekkers, and R.F. Zwaal. 1999. Lipid translocation across the plasma membrane of mammalian cells. *Biochim. Biophys. Acta*. 1439:317–330.

Billy, D., G.M. Willems, H.C. Hemker, and T. Lindhout. 1995. Prothrombin contributes to the assembly of the factor Va-factor Xa complex at phosphatidylserine-containing phospholipid membranes. *J. Biol. Chem.* 270:26883–26889.

Bogdanov, M., M. Umeda, and W. Dowhan. 1999. Phospholipid-assisted refolding of an integral membrane protein. Minimum structural features for phosphatidylethanolamine to act as a molecular chaperone. *J. Biol. Chem.* 274:12339–12345.

Brunger, A.T., P.D. Adams, G.M. Clore, W.L. Delano, P. Gros, R.W. Grosse-Kunstleve, J.S. Jiang, J. Kuszewski, M. Nilges, N.S. Pannu, et al. 1998. Crystallography & NMR system: A new software suite for macromolecular structure determination. *Acta Crystallogr. D Biol. Crystallogr.* 54:905–921.

Conner, S.D., and S.L. Schmid. 2003. Regulated portals of entry into the cell. *Nature*. 422:37–44.

de Kruijff, B. 1997. Lipid polymorphism and biomembrane function. *Curr. Opin. Chem. Biol.* 1:564–569.

Derossi, D., A.H. Joliot, G. Chassaing, and A. Prochiantz. 1994. The third helix of the Antennapedia homeodomain translocates through biological membranes. *J. Biol. Chem.* 269:10444–10450.

D'Hondt, K., A. Heese-Peck, and H. Riezman. 2000. Protein and lipid requirements for endocytosis. *Annu. Rev. Genet.* 34:255–295.

Diekert, K., A.I. de Kroon, U. Ahting, B. Niggemeyer, W. Neupert, B. de Kruijff, and R. Lill. 2001. Apocytochrome c requires the TOM complex for translocation across the mitochondrial outer membrane. *EMBO J.* 20:5626–5635.

Emoto, K., N. Toyama-Sorimachi, H. Karasuyama, K. Inoue, and M. Umeda. 1997. Exposure of phosphatidylethanolamine on the surface of apoptotic cells. *Exp. Cell Res.* 232:430–434.

Engelmann, B., B. Schaipp, P. Dobner, M. Stoeckelhuber, C. Kogl, W. Siess, and A. Hermetter. 1998. Platelet agonists enhance the import of phosphatidylethanolamine into human platelets. *J. Biol. Chem.* 273:27800–27808.

Farsad, K., and P. De Camilli. 2003. Mechanisms of membrane deformation. *Curr. Opin. Cell Biol.* 15:372–381.

Gadella, B.M., and R.A.P. Harrison. 2000. The capacitating agent bicarbonate induces protein kinase A-dependent changes in phospholipid behavior in the sperm plasma membrane. *Development*. 127:2407–2420.

Gardai, S.J., D.L. Bratton, C.A. Ogden, and P.M. Henson. 2006. Recognition ligands on apoptotic cells: a perspective. *J. Leukoc. Biol.* 79:896–903.

Geiger, M. 2007. Protein C inhibitor, a serpin with functions in- and outside vascular biology. *Thromb. Haemost.* 97:343–347.

Huntington, J.A., M. Kjellberg, and J. Stenflo. 2003. Crystal structure of protein C inhibitor provides insights into hormone binding and heparin activation. *Structure*. 11:205–215.

Israelachvili, J.N., S. Marcelja, and R.G. Horn. 1980. Physical principles of membrane organization. *Q. Rev. Biophys.* 13:121–200.

Itoh, T., S. Koshiba, T. Kigawa, A. Kikuchi, S. Yokoyama, and T. Takenawa. 2001. Role of the ENTH domain in phosphatidylinositol-4,5-bisphosphate binding and endocytosis. *Science*. 291:1047–1051.

Iwamoto, K., T. Hayakawa, M. Murate, A. Makino, K. Ito, T. Fujisawa, and T. Kobayashi. 2007. Curvature-dependent recognition of ethanolamine phospholipids by duramycin and cinnamycin. *Biophys. J.* 93:1608–1619.

Jacobson, K., O.G. Mouritsen, and R.G.W. Anderson. 2007. Lipid rafts: at a crossroad between cell biology and physics. *Nat. Cell Biol.* 9:7–14.

Joliot, A., and A. Prochiantz. 2004. Transduction peptides: from technology to physiology. *Nat. Cell Biol.* 6:189–196.

Koonen, D.P.Y., J.F.C. Glatz, A. Bonen, and J.J.F.P. Luiken. 2005. Long-chain fatty acid uptake and FAT/CD36 translocation in heart and skeletal muscle. *Biochim. Biophys. Acta*. 1736:163–180.

Kuwana, T., M.R. Mackey, G. Perkins, M.H. Ellisman, M. Latterich, R. Schneiter, D.R. Green, and D.D. Newmeyer. 2002. Bid, Bax, and lipids cooperate to form supramolecular openings in the outer mitochondrial membrane. *Cell*. 111:331–342.

Liu, Y., M. Jones, C.M. Hingtgen, G. Bu, N. Laribee, R.E. Tanzi, R.D. Moir, A. Nath, and J.J. He. 2000. Uptake of HIV-1 tat protein mediated by low-density lipoprotein receptor-related protein disrupts the neuronal metabolic balance of the receptor ligands. *Nat. Med.* 6:1380–1387.

Mäe M., and U. Langel. 2006. Cell-penetrating peptides as vectors for peptide, protein and oligonucleotide delivery. *Curr. Opin. Pharmacol.* 5:509–514.

Malleier, J., O. Oskolkova, V. Bochkov, I. Jerabek, B. Sokolikova, T. Perkmann, J. Breuss, B.R. Binder, and M. Geiger. 2007. Regulation of protein C inhibitor (PCI) activity by specific oxidized and negatively charged phospholipids. *Blood*. 109:4769–4776.

Marguet, D., M.-F. Luciani, A. Moynault, P. Williamson, and G. Chimini. 1999. Engulfment of apoptotic cells involves the redistribution of membrane phosphatidylserine on phagocyte and prey. *Nat. Cell Biol.* 1:454–456.

Matsuzaki, K., O. Murase, N. Fujii, and K. Miyajima. 1995. Translocation of a channel-forming antimicrobial peptide magainin 2, across lipid bilayers by forming a pore. *Biochemistry*. 34:6521–6526.

Matsuzaki, K., K. Sugishita, N. Ishibe, M. Ueha, S. Nakata, K. Miyajima, and R.M. Epand. 1998. Relationship of membrane curvature to the formation of pores by magainin 2. *Biochemistry*. 37:11856–11863.

McMahon, H.T., and J.L. Gallop. 2005. Membrane curvature and mechanisms of dynamic cell membrane remodelling. *Nature*. 438:590–596.

Morrot, G., P. Herve, A. Zachowski, P. Fellmann, and P.F. Devaux. 1989. Aminophospholipid translocase of human erythrocytes: phospholipid substrate specificity and effect of cholesterol. *Biochemistry*. 28:3456–3462.

Navarro, J., J. Chabot, K. Sherrill, R. Aneja, S.A. Zahler, and E. Racker. 1985. Interaction of duramycin with artificial and natural membranes. *Biochemistry*. 24:4645–4650.

Nishioka, J., M. Ning, T. Hayashi, and K. Suzuki. 1998. Protein C inhibitor secreted from activated platelets efficiently inhibits activated protein C on phosphatidylethanolamine of platelet membrane and microvesicles. *J. Biol. Chem.* 273:11281–11287.

Prendes, M.J., E. Bielek, M. Zechmeister-Machhart, E. Vanyek-Zavadil, V.A. Carroll, J. Breuss, B.R. Binder, and M. Geiger. 1999. Synthesis and ultrastructural localization of protein C inhibitor in human platelets and megakaryocytes. *Blood*. 94:1300–1312.

Priglinger, U., M. Geiger, E. Bielek, E. Vanyek, and B.R. Binder. 1994. Binding of urinary protein C inhibitor to cultured human epithelial kidney tumor cells (TCL-598). The role of glycosaminoglycans present on the luminal cell surface. *J. Biol. Chem.* 269:14705–14710.

Schwarz, G., and A. Arbuzova. 1995. Pore kinetics reflected in the dequenching of a lipid vesicle entrapped fluorescent dye. *Biochim. Biophys. Acta*. 1239:51–57.

Sillerud, L.O., and R.E. Barnett. 1982. Lack of transbilayer coupling in phase transitions of phosphatidylcholine vesicles. *Biochemistry*. 21:1756–1760.

Simons, K., and W.L. Vaz. 2004. Model systems, lipid rafts, and cell membranes. *Annu. Rev. Biophys. Biomol. Struct.* 33:269–295.

Smirnov, M.D., D.A. Ford, C.T. Esmon, and N.L. Esmon. 1999. The effect of membrane composition on the hemostatic balance. *Biochemistry*. 38:3591–3598.

Stoeckelhuber, M., P. Dobner, P. Baumgartner, J. Ehlert, E. Brandt, R. Mentele, D. Adam, and B. Engelmann. 2000. Stimulation of cellular sphingomyelin import by the chemokine connective tissue-activating peptide III. *J. Biol. Chem.* 275:37365–37372.

Takeshima, K., A. Chikushi, K.K. Lee, S. Yonehara, and K. Matsuzaki. 2003. Translocation of analogues of the antimicrobial peptides magainin and buforin across human cell membranes. *J. Biol. Chem.* 278:1310–1315.

Urban, S., S. Zieseniss, M. Werder, H. Hauser, R. Budzinski, and B. Engelmann. 2000. Scavenger receptor BI transfers major lipoprotein-associated phospholipids into the cells. *J. Biol. Chem.* 275:33409–33415.

Vance, J.E. 2003. Molecular and cell biology of phosphatidylserine and phosphatidylethanolamine metabolism. *Prog. Nucleic Acid Res. Mol. Biol.* 75:69–111.

van Klompenburg, W., M. Paetzel, J.M. de Jong, R.E. Dalbey, R.A. Demel, G. von Heijne, and B. de Kruijff. 1998. Phosphatidylethanolamine mediates insertion of the catalytic domain of leader peptidase in membranes. *FEBS Lett.* 431:75–79.

Wang, P.Y., and R.S. Munford. 1999. CD14-dependent internalization and metabolism of extracellular phosphatidylinositol by monocytes. *J. Biol. Chem.* 274:23235–23241.

Wirtz, K.W. 1997. Phospholipid transfer proteins revisited. *Biochem. J.* 324:353–360.

Zieseniss, S., S. Zahler, I. Muller, A. Hermetter, and B. Engelmann. 2001. Modified phosphatidylethanolamine as the active component of oxidized low density lipoprotein promoting platelet prothrombinase activity. *J. Biol. Chem.* 276:19828–19835.

Zwaal, R.F., and A.J. Schroit. 1997. Pathophysiologic implications of membrane phospholipid asymmetry in blood cells. *Blood*. 89:1121–1132.